Reaction Path of UV Photolysis of Matrix Isolated Acetyl Cyanide: Formation and Identification of Ketenes, Zwitterion, and Keteneimine Intermediates

Z. Guennoun,[†] I. Couturier-Tamburelli,[†] S. Combes,[‡] J. P. Aycard,[†] and N. Piétri*[,†]

Laboratoire de Physique des Interactions Ioniques et Moléculaires, UMR 6633 Équipe de Spectrométries et Dynamique Moléculaires, Université de Provence, Centre de St-Jérôme case 252, 13397 Marseille Cedex 20, France, and Laboratoire de Chimie, Biologie et radicaux libres, UMR 6517, Université de Provence, Centre de St-Jérôme case 541, 13397 Marseille Cedex 20, France

Received: July 6, 2005; In Final Form: August 30, 2005

Irradiations at $\lambda > 180$ nm and $\lambda > 230$ nm of CH_3COCN (CD_3COCN) trapped in an argon matrix at 10 K have been performed and monitored by Fourier transform infrared spectroscopy. For both wavelengths, the first photoreaction product is acetyl isocyanide. At $\lambda > 180$ nm acetonitrile and methyl isocyanide are obtained as final products. They are formed by photolysis of acetyl isocyanide and acetyl cyanide, respectively. Unstable intermediates, such as ketene:HCN and ketene:HNC complexes, H_2CNCH zwitterion, and H_2C_2NH keteneimine, not observed in the gas phase, are trapped and identified at our experimental temperature. The complexes have an L-shaped structure with a hydrogen bond between the oxygen atom of ketene and the hydrogen atom of HCN or HNC. A pathway process is proposed and compared with the ones determined in the ground state by ab initio calculations.

Introduction

Acetyl cyanide, CH_3COCN, is a molecule of considerable chemical interest. It is an asymmetrically substituted carbonyl compound, and the characteristics of the two C−C chemical bonds, adjacent to the C═O group, are expected to be quite different from each other. Structural determinations of gaseous acetyl cyanide began with the 1959 report of Krisher et al.[1] and have been carried out with gas-phase electron diffraction work[2] and further spectroscopic studies.[3,4] Vibrational frequencies have been evaluated from ab initio calculations using Hartree−Fock wave functions.[4]

The thermal unimolecular reaction of acetyl cyanide has been investigated both experimentally[5−7] and theoretically.[6,8,9] Three reaction channels have been considered:

$$CH_3COCN \rightarrow CO + CH_3CN\ (CH_3NC) \quad (1)$$

$$CH_3COCN \rightarrow CH_2CO + HCN \quad (2)$$

$$CH_3COCN \rightleftharpoons CH_3CONC \quad (3)$$

Bennet et al.[7] reported that the reaction obtained by pyrolysis at 743 K of acetyl cyanide proceeds predominantly via decarbonylation: eq 1. However, scission to ketene (CH_2CO) and hydrogen cyanide (HCN) was also found to be competitive. Okada et al.[6] studied thermal uimolecular reactions of acetyl cyanide diluted in Ar behind shock waves. Gas chromatographic analysis revealed an absence of reaction products at temperatures <1200 K. Decomposition products, such as ketene, were clearly detected above 1350 K, but they had not observed acetonitrile (CH_3CN), one of the products of decomposition obtained by Bennet et al.[7] Okada et al.[6] performed ab initio calculations and showed that the unimolecular decompositions are energetically less favorable compared to the isomerization leading to acetyl isocyanide CH_3CONC (eq 3).

Since 1997, several groups[10] have investigated experimentally the photodissociation of acetyl cyanide at 193 nm and have got consistent observations. The major product of acetyl cyanide photolysis was found to be the $CN^•$ radical. This result was explained by a cleavage of either nonequivalent α_{C-C} bonds with the pathway (4) that is predominant.

$$CH_3COCN \rightarrow CH_3CO + CN \quad (4)$$

$$CH_3COCN \rightarrow CH_3 + COCN \quad (5)$$

Photoabsorption spectra of acetyl cyanide have been measured in the 150−400 nm range,[10b−d] and assignment of the lower energy transition has been made on the basis of ab initio MO calculations.[11] A weak band with coarse vibronic structure centered at ∼300 nm was assigned to the S1 ($n\pi^*$) transition localized on the CO group. The onset of the second weak absorption band near 230 nm and successive strong bands starting from 200 nm to the shorter wavelengths were attributed to S2 (π_{CN}, π^*_{CO}) and S3 (π_{CO-CN}, π^*_{CO}) transitions, respectively.

The photodissociation of gaseous acetyl cyanide at 193 nm have been initiated by the direct excitation of the S3 state.[10] Only Aoyama et al.[12] have studied this photodissociation by multiphoton UV absorption at 292 nm using S1 as the resonance state. In the two cases, it has been shown that acetyl cyanide is the most efficient source of $CN^•$ radical. Indeed, the dissociation leading to $CN^• + CH_3CO^•$ is the main decay path (85%), $CH_3CO^•$ is not stable and exhibits spontaneous fragmentation of the acetyl fragments $CH_3 + CO$ with a yield of 9%.

* Corresponding author. Telephone: 33(0)491282816. Fax: 33(0)-491636510. E-mail: nathalie.pietri@up.univ-mrs.fr.

[†] Laboratoire de Physique des Interactions Ioniques et Moléculaires, Université de Provence.

[‡] Laboratoire de Chimie, Biologie et radicaux libres, Université de Provence.

10.1021/jp0536854 CCC: $30.25
Published on Web 11/22/2005

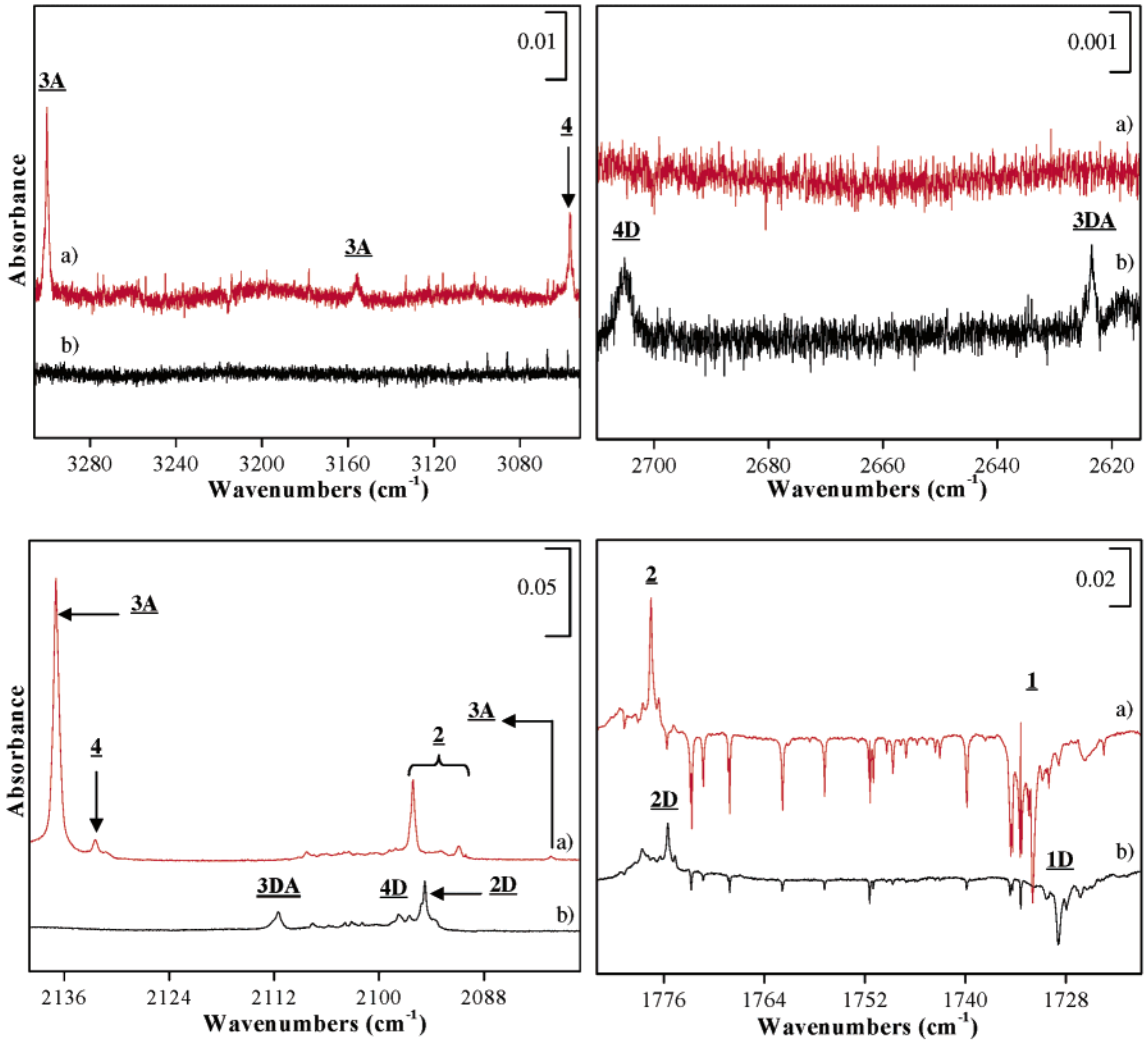

Figure 1. Subtraction FTIR spectra (spectrum after 56 h of irradiation − spectrum after deposition) of (a) CH_3COCN and (b) CD_3COCN, respectively, photolyzed at $\lambda > 230$ nm in argon matrix at 10 K.

TABLE 1: Formulas and Labeling of the Initial Product and Species Obtained during the Respective Irradiations of CH_3COCN and CD_3COCN

products	label	products	label
CH_3COCN	**1**	CD_3COCN	**1D**
CH_3CONC	**2**	CD_3CONC	**2D**
ketene:HCN complexes	**3A**, **3B**, **3C**	D_2-ketene:DCN complexes	**3DA**, **3DB**, **3DC**
ketene:HNC complex	**4**	D_2-ketene:DNC complex	**4D**
zwiterrion $HCNCH_2$	**5**	zwiterrion $DCNCD_2$	**5D**
keteneimine H_2C_2NH	**6**	keteneimine D_2C_2ND	**6D**
acetonitrile CH_3CN	**7**	acetonitrile CD_3CN	**7D**
methyl isocyanide CH_3NC	**8**	methyl isocyanide CD_3NC	**8D**

In the present study, we report for the first time experimental results on the photochemical decomposition of acetyl cyanide trapped in argon cryogenic matrix at 10 K. This technique allows us to trap intermediates, not observed in the gas phase, and to provide more details about the experimental pathways from acetyl cyanide to acetonitrile. We performed irradiations of different isotopomers at distinct wavelengths to select the electronic absorption bands.

Experimental Section

Acetyl cyanide, **1** (from Aldrich (95%)), was used after purification by vacuum distillation. CD_3COCN, **1D**, was prepared as follows from the corresponding acetyl chloride by reaction with trimethylsilyl cyanide and zinc iodide as catalyst.[13] Under argon, at 10 °C, to a suspension of ZnI_2 (212 mg, 0.67 mmol) in Me_3SiCN (7.46 mL, 56 mmol) was added drop by drop CD_3COCl (4.0 mL, 56 mmol). After stirring for 1 h at 0 °C, to ensure complete reaction, the mixture was purified by fractional distillation under argon atmosphere to afford CD_3-COCN (3.86 g, 96%) as a brown oil (bp 93 °C).

The apparatus and experimental techniques used to obtain the argon matrix have been described elsewhere.[14] The matrix was obtained by spraying a 1/500 mixture of **1** or **1D** in argon onto a golden copper plate cooled at 20 K. The samples were then cooled at 10 K and spectra were recorded in transmission using a Fourier transform infrared spectrometer (Nicolet Series II Magna System 750) from 4000 to 650 cm^{-1}, with a resolution of 0.125 cm^{-1}.

TABLE 2: Observed and Simulated Vibrational Frequencies (cm^{-1}) (Scaled with 0.96 Factor) of Acetyl Cyanide 1, 1D, and Acetyl Isocyanide 2, 2D

	CH_3COCN		CD_3COCN		$\Delta\nu$[a]	
assignment	ν_{calcd}(I)	ν_{exptl}(I)	ν_{calcd}(I)	ν_{exptl}(I)	calcd	exptl
ν_{CH}	3046.6 (2)	3031.7 (<1)	2260.0 (<1)		786.6	
	2991.2 (1)	2979.0 (<1)	2213.3 (<1)		777.9	
	2928.5 (<1)	2931.3 (2)	2104.6 (<1)	2123.9 (<1)	823.9	807.4
ν_{CN}	2248.5 (16)	2225.6 (32)	2249.5 (15)	2227.8 (18)	−1.0	−2.2
ν_{CO}	1736.7 (100)	1732.1 (100)	1733.0 (100)	1729.0 (100)	3.7	3.1
β_{CH_2}	1418.6 (11)	1426.1 (26)	1022.7 (7)	1036.9 (5)	395.9	389.2
	1411.8 (10)	1399.6 (3)	1022.3 (3)	1035.3 (3)	389.5	364.3
	1345.6 (24)	1364.5 (28)	999.1 (20)	1022.0 (14)	346.5	342.5
β_{CCH}	1154.0 (85)	1175.8 (89)	1159.0 (93)	1178.5 (65)	−5.0	−2.7
	1006.0 (4)	1023.3 (7)	874.1 (1)	891.4 (4)	131.9	131.9
	948.0 (15)	972.5 (15)	806.1 (1)	828.6 (<1)	141.9	143.9
ν_{CC}	691.4 (16)	707.3 (23)	638.9 (10)	655.8 (10)	52.5	51.5
	CH_3CONC		CD_3CONC		$\Delta\nu$[a]	
assignment	ν_{calcd}(I)	ν_{exptl}(I)	ν_{calcd}(I)	ν_{exptl}(I)	calcd	exptl
ν_{CH}	3052.4 (≪1)		2266.1 (<1)		786.3	
	2938.0 (≪1)		2221.7 (≪1)		716.3	
	3002.0 (≪1)		2111.4 (≪1)		890.6	
ν_{NC}	2089.6 (100)	2096.1 (100)	2089.6 (100)	2094.9 (100)	0	1.2
ν_{CO}	1771.3 (70)	1777.5 (77)	1767.9 (71)	1775.6 (52)	3.4	1.9
β_{CH_2}	1423.6 (2)		1025.8 (1)		397.8	
	1416.0 (4)		1025.3 (6)		390.7	
	1349.7 (10)	1369.2 (11)	999.3 (19)	1011.7 (12)	350.4	357.5
β_{CCH}	1145.2 (60)	1155.4 (26)	1153.9 (61)	1171.4 (29)	−8.7	−16.0
	1018.6 (2)	1038.9 (3)	881.4 (3)	902.6(≪1)	137.2	136.3
	959.9 (13)	985.0 (21)	813.1 (1)	835.9 (≪1)	146.8	149.1
ν_{CC}	718.5 (13)	724.0 (8)	668.3 (9)	678.5 (11)	50.2	45.5

[a] $\Delta\nu$ (exptl or calcd) = ν(1) − ν(1D).

TABLE 3: Experimental and Theoretical Frequency Shifts (cm^{-1}) for the A, B, and C Complexes of Ketene:HCN 3

	ν_{exptl}				ν_{calcd}			$\Delta\nu_{exptl}$[a]			$\Delta\nu_{calcd}$[a]	
	isolated	complexed **3A**	complexed **3B**	complexed **3C**	isolated	L	T	**3A**	**3B**	**3C**	L	T
ketene[b]	3062	3056.5 (7)	3048.6 (100)	3060.4 (14)	3205 (5)	3202 (7)	3196 (6)	−5.5	−13.4	−1.6	−3	−9
	2142	2136.9 (100)		2139.8 (100)	2240 (100)	2232 (100)	2242 (100)	−5.1		−2.2	−8	2
	1381	1375.8 (3)		1377.6 (1)	1425 (3)	1422 (2)	1422 (4)	−5.2		−3.4	−3	−3
	1115	1123.6 (1)		1130.9 (<1)	1176 (1)	1178 (3)	1172 (<1)	8.6		15.9	2	−4
	974				992 (1)	987 (2)	998 (<1)				−5	6
HCN[c]	3306	3300.1 (18)	3295.5 (40)	3268.5 (35)	3476 (100)	3418 (51)	3362 (59)	−5.9	−10.5	−37.5	−58	−114
	2098	2080.0 (1)		2092.6 (15)	2212 (4)	2208 (20)	2201 (13)	−18.0		−5.4	−4	−11
	721	725.5 (6)		792.0 (32)	769 (64)	849 (6)	863 (4)	4.5		71.0	80	94
	ν_{exptl}				ν_{calcd}			$\Delta\nu_{exptl}$[a]			$\Delta\nu_{calcd}$[a]	
		3DA	**3DB**	**3DC**				**3DA**	**3DB**	**3DC**		
D_2-ketene[b]	2263	2255.4 (19)	2248.1 (16)	2258.7 (44)	2357 (52)	2356 (54)	2348 (56)	−7.5	−14.9	−4.3	−1	−9
	2113	2111.5 (100)	2117.2 (20)	2114.6 (100)	2207 (100)	2199 (100)	2212 (100)	−1.5	4.2	1.6	−8	5
	1225	1224.6 (<1)			1267 (<1)	1270 (≪1)	1262 (1)	−0.4			3	−5
	920	921.0 (2)			933 (3)	932 (3)	934 (2)	1.0			−1	1
	849	849.4 (2)			864 (2)	860 (2)	865 (2)	0.4			−4	1
DCN[c]	2631.3	2623.6 (15)	2618.6(100)	2605.5 (15)	2755 (100)	2725 (21)	2700 (27)	−7.7	−12.7	−25.8	−30	−55
	1922.7	1924.1 (4)	1913.2 (3)	1914.3 (7)	2011 (39)	1996 (19)	1976 (22)	1.4	−9.5	−8.4	−15	−35
	572.0				613 (50)	669 (2)	673 (2)				56	60

[a] $\Delta\nu$ = ν(complex) − ν(monomer). [b] Reference 16. [c] Reference 17.

The samples were irradiated using a microwave discharge hydrogen flow lamp (Opthos Instrument). The lamp UV flux transmitted through a quartz window (λ >180 nm) was considered in the range from 3 to 10 eV. The operating pressure of the lamp was 0.9 mbar. Irradiations of **1** and **1D** were also performed using an Osram 200 W high-pressure mercury lamp equipped with a quartz envelope. The broad band was filtered at λ > 230 nm.

The vibrational spectra of the reaction products (acetyl isocyanide and ketene:HCN (HNC)) were determined by DFT (density functional theory) calculations. The Gaussian 03[15] program package using B3LYP procedure with 6-31G** basis set was used for these calculations.

Results

When acetyl cyanide **1** (Table 1), isolated in matrix, was irradiated at λ > 230 nm in its n → π^*(S1) absorption band, we observed a decrease of **1** absorption bands and new bands appeared in different areas of the spectrum (Figure 1). The evolution of the integrated absorbances versus time permitted us to distinguish three sets of bands. The most intense of the first set were observed at 2096.1 and 1777.5 cm^{-1} and are

TABLE 4: Experimental and Theoretical Frequency Shifts (cm^{-1}) for the Ketene:HNC 4 and D_2-Ketene:DNC 4D Complexes

	ν_{exptl}		ν_{calcd}				$\Delta\nu_{calcd}$[a]	
	isolated	complexed	isolated	L	T	$\Delta\nu_{exptl}$[a]	L	T
ketene[b]	3062	3062.8 (8)	3205 (5)	3201 (4)	3189 (3)	0.8	−4	−16
	2142	2132.3 (100)	2240 (100)	2227 (70)	2243 (55)	−9.7	−13	3
HNC[c]	3620	3506.0 (3)	3835 (100)	3688 (100)	3561 (100)	−114	−147	−274
	2029	2029.6 (12)	2114 (25)	2119 (1)	2110 (1)	0.6	5	−4
D_2-ketene[b]	2263	2261.3/2260.1 (12)	2357 (52)	2355 (45)	2342 (37)	−1.7/−2.9	−2	−15
	2113	2098.6 (37)	2207 (100)	2194 (85)	2215 (66)	−14.4	−13	8
DNC[c]	2769	2705.0 (100)	2900 (100)	2807 (100)	2733 (100)	−64.0	−93	−167
	1940	1935.0/1933.4 (8)	2013 (14)	2006 (1)	1982 (2)	−5.0/−6.6	−7	−31

[a] $\Delta\nu = \nu$(complex) − ν(monomer). [b] Reference 16. [c] Reference 18.

TABLE 5: Experimental Frequencies (cm^{-1}) of 5, 5D, 6, and 6D Obtained from Acetyl Cyanide 1 and 1D Photolysis at $\lambda > 180$ nm

species	frequencies (cm^{-1})		species	frequencies (cm^{-1})		$\Delta\nu$[a]	
	this work	literature[b]		this work	literature[b]	this work	literature
H_2CCNH, **6**	2039.9 (100)	2040 (vs)	D_2CCND, **6D**	1997.7 (100)	1998 (vs)	42.2	42
		1124 (w)			921 (m)		
	992.7 (30)	1000 (s)		806.8 (49)	800 (s)		
	882.8 (24)	872 (m)			648 (m)		
	689.3 (18)	690 (m)					
species	frequencies (cm^{-1})		species	frequencies (cm^{-1})		$\Delta\nu$[a]	
	this work	literature[c]		this work	literature[d]	this work	literature
H_2CNCH, **5**	1915.1 (50)	1914.5 (s)	D_2CNCD, **5D**	1870.7 (100)	1870.2 (vs)	44.4	44.3
		1183.6 (w)			982.6 (w)		
		1127.3 (w)			900.1 (w)		
	867.3 (100)	866.3 (vs)		707.6 (52)	708.3 (ms)		

[a] $\Delta\nu = \nu_{5(6)} - \nu_{5D(6D)}$. [b] Reference 20. [c] Reference 19. [d] Reference 19a.

characteristic of $\nu_{N\equiv C}$ and $\nu_{C=O}$ stretching modes, respectively (Figure 1). These bands could be attributed to acetyl isocyanide **2** (Table 1), which has not been characterized by experimental spectroscopic data. To confirm this identification, we performed irradiation of CD_3COCN at $\lambda > 230$ nm and harmonic vibrational frequency calculations.

The results given in Table 2 show good agreement between experimental and theoretical frequencies.

In the second group of bands listed in Table 3, those observed at 2136.9 and 2080.0 cm^{-1} (Figure 1) could be attributed, in agreement with literature data, to the ν_{CCO} mode of CH_2CO and the $\nu_{C\equiv N}$ mode of HCN molecule, respectively. The ketene molecule, trapped in argon matrix, is characterized in infrared by a strong absorption band at 2142 cm^{-1} (ν_{CCO}).[16] The CN stretching modes of HCN[17] and HNC[18] molecules are observed in argon at 2098 and 2029 cm^{-1}, respectively. However, in our experiments, the absorption bands observed at 2136.9 and 2080 cm^{-1} are shifted by 5.1 and 18.0 cm^{-1} toward lower frequencies with respect to the ν_{CCO} mode of ketene monomer and the ν_{CN} mode of HCN monomer, respectively (Table 3). Therefore, we can assume that these frequency shifts are due to the formation of a complex between the ketene and HCN trapped in the same cage. The isotopomer experiment confirms this hypothesis, and the results are reported in Table 3.

In the last group of bands, we observed four bands (Figure 1) at 3062.8, 2132.3, 3506.9, and 2029.6 cm^{-1} (Table 4) assigned, by analogy with the conclusion cited above, to the ν_{CH}, ν_{CCO}, ν_{HN}, and $\nu_{N\equiv C}$ modes of ketene:HNC complex. Indeed, the shifts observed between these vibrational frequencies and those of the monomers in the two isotopomer experiments allow us to conclude a ketene:HNC complex formation (Table 4).

These experimental shifts show that the complexes ketene:HCN and ketene:HNC do not have the same geometric structure. We noted the complex ketene:HCN **3A** (Table 3) and the complex ketene:HNC **4** (Table 4). Moreover, the evolution of the ν_{CCO} integrated absorbance of the CH_2CO bands of the complexes versus time shows that the **3A** complex is formed in greater amount than the **4** one. At the end of irradiation, the absorbance ratio $A[\nu_{CCO}(\mathbf{3A})]/A[\nu_{CCO}(\mathbf{4})] = 10$. Although the isomerization between the two complexes is possible, more toward **3A**, we can admit that the principal photochemical process from acetyl cyanide **1** irradiation at $\lambda > 230$ nm is the **3A** complex formation.

When matrix isolated **1** and **1D** are irradiated at $\lambda > 180$ nm in $n\pi^*$ (S1 and S2) and $\pi\pi^*$(S3) transitions, we observe first, as in the previous photolysis experiments ($\lambda > 230$ nm), the decrease of **1** absorption bands and the growth of **2**, **3A**, and **4** absorption bands. Nevertheless, at these wavelengths we observe for the complex ketene:HCN two groups of bands indicating the formation of two different complexes: **3A**, already observed after **1** irradiation at $\lambda > 230$ nm, and a second complex denoted **3B**. Their frequencies are reported in Table 3.

Second, **2** and the complexes **3** (**3A** and **3B**) and **4** undergo photolysis and their absorption bands start to decrease in intensity after 4 h of irradiation. New strong absorption bands (Table 5) grow at 1915.1 and 2039.9 cm^{-1} and behave as a reaction intermediate (Figure 2). According to Maier et al.[19a] and Jacox et al.,[20] we can assign these bands to the ν_3 (ν_{CNC} and ν_{CCN}) mode of zwitterion $HCNCH_2$ **5** and keteneimine H_2C_2-NH **6**, respectively. In the isotopomer experiment, these modes are shifted toward lower frequencies by 42.2 and 44.4 cm^{-1}, respectively. These shifts are in good agreement with literature data (42.0 and 44.3 cm^{-1}) and confirm the formation of **5** and **6**. All other bands of these two compounds compared to literature data are reported in Table 5. At the same time of irradiation other bands grow at 2133.7 and 2143.0 cm^{-1} which behave in the same way as the bands of keteneimine and

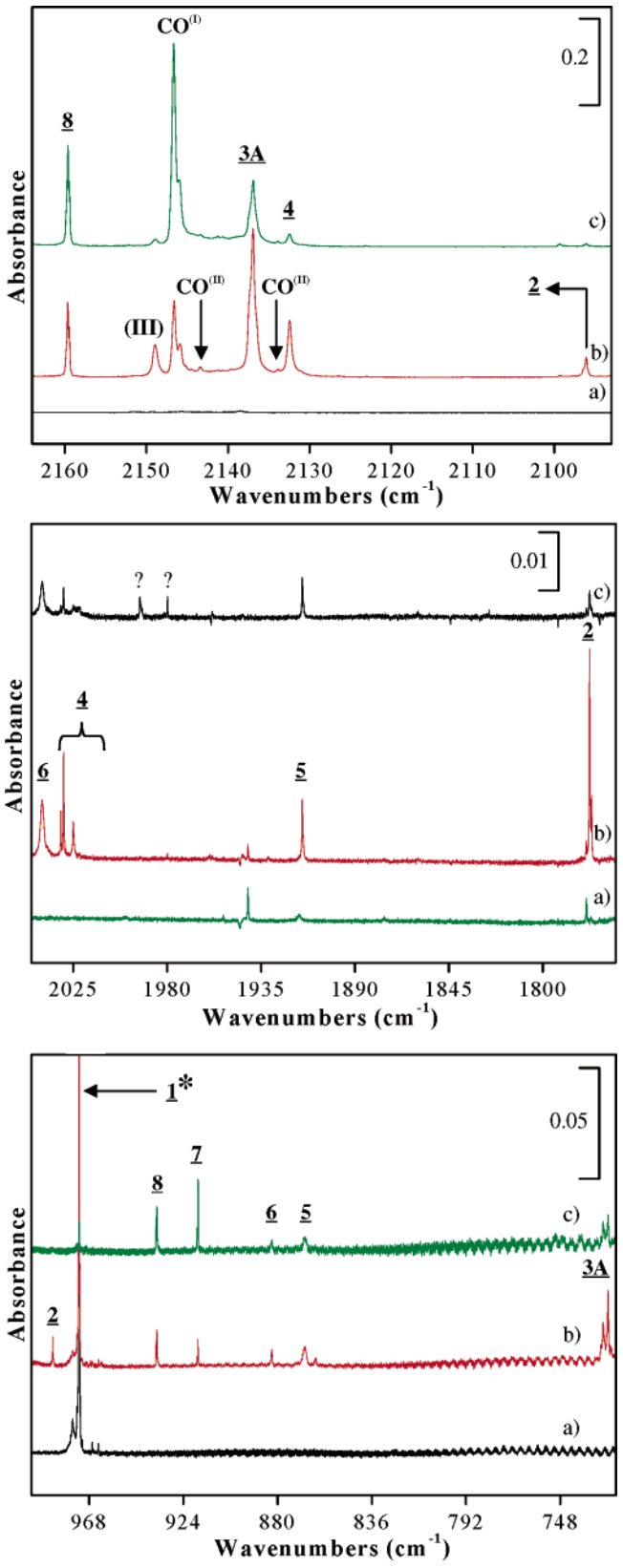

Figure 2. Evolution of FTIR spectra at 10 K of acetyl cyanide **1** during irradiation at $\lambda > 180$ nm: (a) spectrum after deposition; (b) spectrum after 4 h of irradiation; (c) spectrum after 19 h of irradiation. The band denoted with an asterisk (*) was saturated to enhance the medium and weak bands. (I) Band of CO complexed with acetonitrile; (II) bands of CO complexed with zwitterion and keteneimine; (III) band probably due to an another ketene:HNC complex, but only one band was observed for this structure.

SCHEME 1: Probable Reaction Pathways for the Photolysis Products Obtained by Irradiation of 1 at $\lambda > 180$ nm

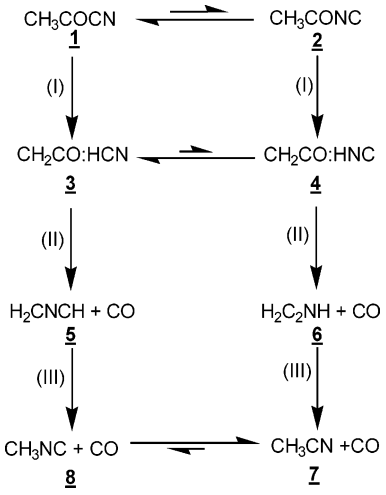

zwitterion (Figure 2). These two bands, which are not modified in the isotopomer experiment, could be attributed to the CO molecule[21] observed isolated in argon matrix at 2138 cm^{-1}. Indeed, the zwitterion and the keteneimine coming from the photodecomposition of complexes **3** and **4**, respectively, are trapped with CO in the same argon cage. The interaction between the two molecules (keteneimine and CO or zwitterion and CO) explain the differences observed between our results and the frequencies of isolated molecules in argon matrix.

In the last step, we observed the increase of bands reported in Table 6 which could be attributed unambiguously to the CH_3-CN **7** and CH_3NC **8** molecules[22] (Figure 2). The comparison between the bands of **7** obtained after photolysis of **1** and those obtained after deposition of **7** isolated in argon matrix shows slight shifts. These shifts and that one observed for the $\nu_{C\equiv O}$ frequency (8.5 cm^{-1}) which appears at 2146.5 cm^{-1} are due to the interaction between these two molecules trapped in the same cage. Acetonitrile **7** and methyl isocyanide **8** probably come from a rearrangement of the keteneimine **6** and zwitterion **5**, respectively. Finally, the evolution of the integrated absorbances versus time of **7** and **8** absorption bands shows an isomerization process between these two molecules, more toward **7**.

Discussion

Photolysis of Acetyl Cyanide 1 and Acetyl Isocyanide 2: Step I (Scheme 1). *Photolysis Results.* Photolysis of **1** shows the formation of different primary and secondary products. Whatever the irradiation wavelengths, the first product obtained is the acetyl isocyanide **2**. Our results are in agreement with literature data[6,9] reporting that the isomerization of acetyl cyanide is reversible and the most favorable process. Sumathi et al.[9] have modeled this reaction in the ground state, and the energy barrier was found to be only 41 kcal/mol. Furthermore, the first experimental report of the photodissociation of gaseous acetyl cyanide at 193 nm[10a] put in evidence CN radical formation. In our experiment, the two radicals (CH_3CO and CN) are trapped in the same argon cage, allowing the recombination and isomerization processes to occur.

The easiest molecular dissociation channel from acetyl cyanide **1** calculated by Sumathi et al.[9] is the 1,2 elimination of HCN with the formation of ketene CH_2CO (E_a = 65 kcal/mol). The same HNC elimination activation barrier from acetyl

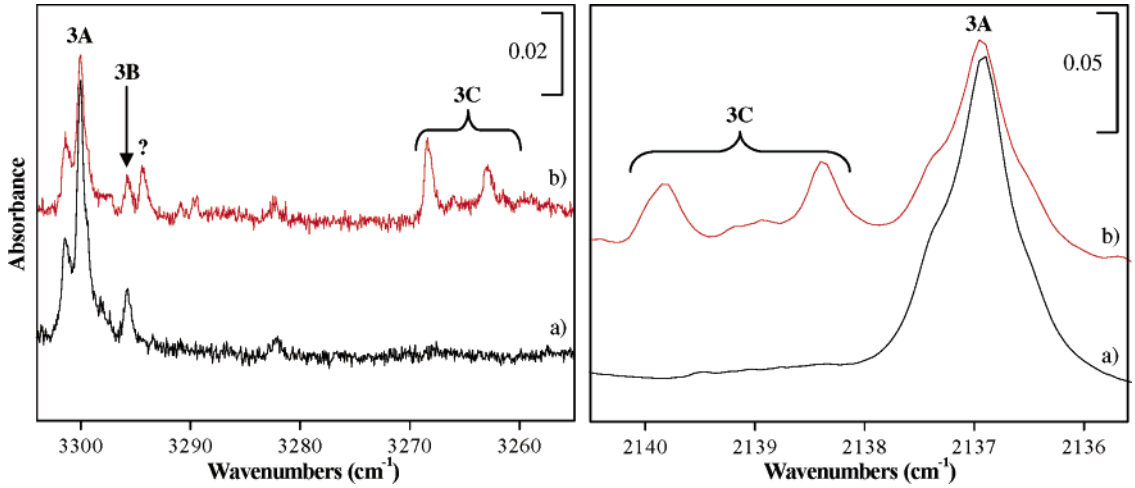

Figure 3. Evolution of FTIR spectra of bands of the ketene:HCN complex during annealing experiment: (a) 10 K after 19 h of irradiation at $\lambda >$ 180 nm; (b) 10 K after 35 K.

TABLE 6: Experimental Frequencies (cm^{-1}) of 7, 7D, 8, and 8D Obtained from Acetyl Cyanide 1 and 1D Photolysis at $\lambda >$ 180 nm

	ν_{CH_3CN}(7)		ν_{CD_3CN}(7D)		ν_{CH_3NC}(8)		ν_{CD_3NC}(8D)	
assignments	this work	literature[a]	this work	literature[a]	this work	literature[a]	this work	literature[a]
				A_1 Fundamentals				
ν_1 (CH(D) str)	2950.9 (3)	2950.3	2122.0 (6)	2122.1	2959.5 (5)	2959.3	2128.2 (5)	2128.1
ν_2 (CN/NC str)	2256.8 (21)	2258.4	2266.1 (100)	2267.3	2159.7 (100)	2160.6	2160.1 (100)	2160.8
ν_3 (CH_3 def)	1374.4 (35)	1375.8	1103.8 (23)	1104.7		1421.6	1110.2 (6)	1111.7
ν_4 (CC str)	917.0 (16)	916.9	829.0 (96)	829.1	936.4 (14)	938.0	871.1 (13)	872.2
				E Fundamentals				
ν_5 (CH str)		3004.0		2253.7		3011.0		2259.0
ν_6 (CH_3 def)	1444.8 (100)	1445.0	1038.8 (55)	1040.1	1457.2 (20)	1457.0	1051.1 (1)	1052.2
ν_7 (CH_3 rock)	1038.9 (11)	1037.9	846.4 (69)	845.5		1128.7		890.1

[a] Reference 22.

isocyanide was found to be 50 kcal/mol. The authors explain that the CN fragment first gets detached from the carbonyl carbon and then forms the bond with hydrogen.

An another important unimolecular isomerization that they modeled is the 1,3 hydrogen migration from the methyl group to the carbonyl oxygen of **1**, giving rise to an enol derivative. For CH_3COCN the transition structure state for this process is only 66.4 kcal/mol higher than the ground state. This energy value suggests that the 1,3 hydrogen migration is a competing channel. On the other hand, the barrier for the 1,3 hydrogen migration in acetyl isocyanide is quite high (90 kcal/mol) compared to ketene and HNC products formation. The enol forms are not observed in our experiment. Then we can assume that, for both acetyl cyanide **1** and acetyl isocyanide **2**, the first molecular photodissociation process is the 1,2 elimination of HCN or HNC by breaking of the C−CN (C−NC) bond along with the formation of ketene CH_2CO. The two molecules, trapped in the same cage, lead to the formation of ketene:HCN and ketene:HNC complexes from **1** and **2** photolysis, respectively.

When the matrix is irradiated at $\lambda >$ 180 nm, these complexes undergo photolysis. Before we explain their photochemistry, we have investigated their structures from theoretical calculations.

Identification of the Complexes Ketene:HCN (HNC). To understand the structural differences of the two complexes ketene:HCN and ketene:HNC obtained during irradiation, we performed annealing for both experiments. After 19 h of irradiation at $\lambda >$ 180 nm, warming the matrix to 35 K induces important changes in the IR spectra of complexes (Figures 3 and 4). During annealing, the absorption bands attributed to **3A** and **3B** complexes decrease. Other new absorption bands denoted **3C** increase (Figure 3). In the isotopomer experiment concerning the D_2-ketene:DCN annealing study (Figure 4), we note at 10 K, after a warming at 30 K, the decrease of the **3DA** bands and the increase of those of **3DB** and **3DC**. At 10 K after 35 K the bands of **3DB** decrease and those of **3DC** heighten in intensity. Thus, after an annealing to 35 K, we conclude that the **3A** complex is restructured toward a **3C** structure through the **3B** one, which is an intermediate structure.

To model the complex structures and their vibrational spectra, theoretical calculations were performed on different starting geometries for each complex (B3LYP/6-31G**). The stabilization energy calculations were described elsewhere in the literature.[23] For each energy structure minimum, normal coordinate calculations were done. The resulting vibrational frequencies remained unscaled.

Calculations yield only two minima. The optimized structures are shown in Scheme 2. The first one, denoted the L form, exhibits a hydrogen bond between the oxygen atom of ketene and the hydrogen (or deuterium) atom of HCN (or HNC). The second one is the T form, for which hydrogen bonding occurs with the C_β atom of ketene. Whatever the structure, the ketene:HCN complex is more stable by 14.0 kcal/mol than the ketene:HNC one. For the two complexes, the L form is more stable than the T one by only 0.8 kcal/mol. After BSSE correction, the T and L forms of ketene:HCN complex are stabilized with regard to the monomers molecules by 2.0 and 2.6 kcal/mol, respectively. For ketene:HNC the two forms are stabilized with regard to monomers by 4.0 kcal/mol.

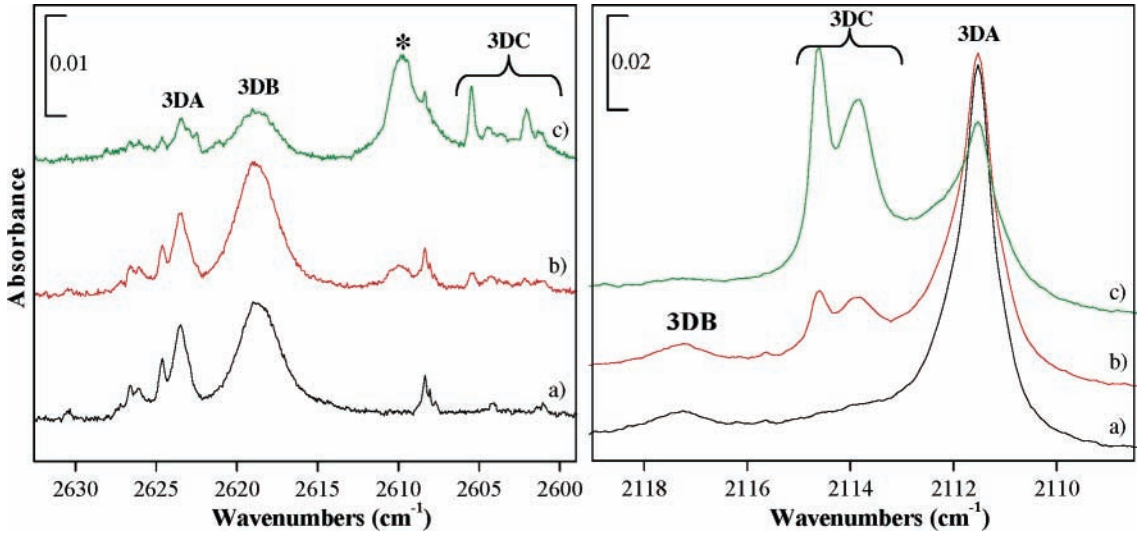

Figure 4. Evolution of FTIR spectra of bands of the D_2-ketene:DCN complex during annealing experiment: (a) 10 K after 29 h of irradiation at $\lambda > 180$ nm; (b) 10 K after 30 K; (c) 10 K after 35 K. The band denoted with an asterisk (*) is probably due to an another ketene:HCN complex. Only one band was observed for this structure.

SCHEME 2: Optimized Geometries of Ketene:HCN and Ketene:HNC Complexes at the B3LYP/6-31G Level of Theory**[a]

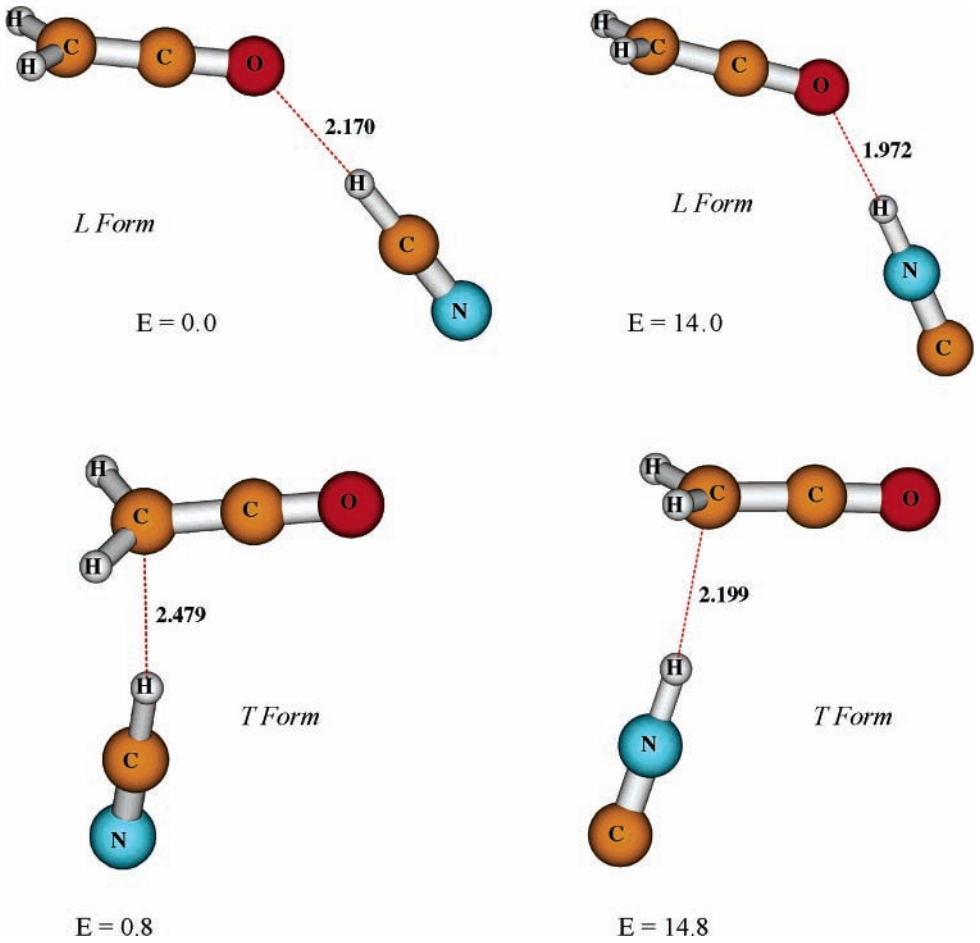

[a] Bond lengths are given in angstroms. Relative energies are given in kilocalories per mole.

The calculated harmonic frequencies of the monomers and those of the complexes ketene:HCN and ketene:HNC are summarized in Tables 3 and 4, respectively.

To identify the form existing in argon matrix, with the energy difference between T and L complexes being too weak, we compare the vibrational frequencies of the two complexes with regard to those of the free molecules. Analysis of Tables 3 and 4 shows differences between the calculated frequencies of the T and L complexes. The calculated red shifts for the ν_{HN} (HNC) or ν_{HC} (HCN) stretching modes are much more important for the T form than those obtained for the L form. The ν_{CCO} stretching modes are shifted toward the lower and higher frequencies with respect to the monomer for the L and T forms, respectively.

SCHEME 3: Reaction and Energetic Pathways for the Rearrangement of Keteneimine to Acetonitrile Calculated by Doughty et al.[25] (MCSCF/DZP)[a]

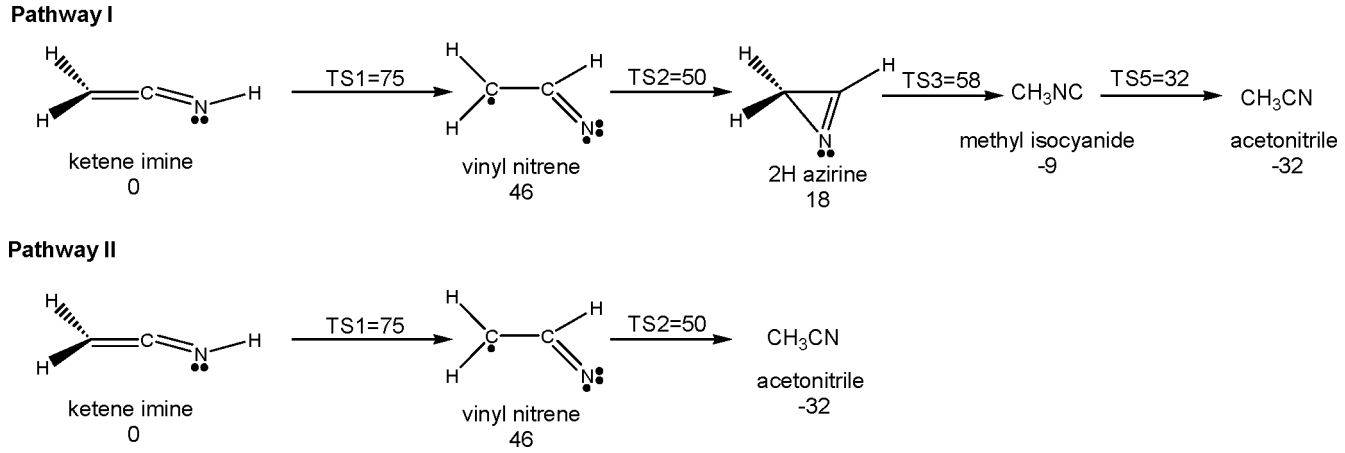

[a] Relative energies are given in kilocalories per mole. TS = transition state.

For the ketene:HNC complex (Table 4), the comparison between the experimental and theoretical shifts allows us to conclude that the complexes ketene:HNC **4** or D_2-ketene:DNC **4D** are formed after irradiation and, whatever the wavelengths, the complexes have a L-shaped structure.

For the ketene:HCN complex, the conclusion is rather different. Indeed, the frequencies of the **3A** complex, observed at the end of the irradiation at $\lambda > 230$ nm (Table 3), show slight shifts with regard to the monomers for most of the modes. The ν_{CH} stretching mode of HCN is only shifted by -5.9 cm^{-1}. This shift is more important for the **3B** structure (-10.5 cm^{-1}). The structure of these complexes could not be identified by comparison with the calculated frequencies of the L and T complex forms. On the other hand, the experimental frequencies of the **3C** complex, obtained after annealing, are in good agreement with those calculated for the L structure (Table 3). At the end of irradiation the ketene and HCN molecules formed are trapped in the same cage but do not really form a complex. When the temperature increases, the reorganization in the cage becomes possible allowing the two molecules to lead to a stable complex, **3C**.

The observation of the L ketene:HNC complex directly after irradiation and the L ketene:HCN complex only after warming can be explained by their stability energies. Indeed, the ketene:HCN complex is only stabilized with regard to the monomers by 2.0 kcal/mol while the ketene:HNC complex is stabilized by 4.0 kcal/mol.

Photolysis of Complexes: Step II (Scheme 1). The photochemistry of ketenes is a classical research problem.[24] Hochstrasser et al.[25] have studied the photolysis of ketene in an Ar matrix, and they showed that the first reaction step is a decarbonylation reaction yielding CO and the carbene CH_2. In our experiment this latter species is present in the same cage with HCN or HNC, which CH_2 can react with. The reaction between these two compounds yields the formation of keteneimine and zwitterion, in interaction with the CO molecule trapped in the same cage. Therefore, we obtained H_2CNCH **5** and H_2C_2NH **6** by photolysis of complexes **3** and **4**, respectively.

Photolysis of Keteneimine and Zwitterion: Step III (Scheme 1). According to literature data,[26,27] several pathways could be considered to rearrange keteneimine to acetonitrile. Doughty et al.[26] proposed two reaction processes. The first one consists of the following series of reactions: keteneimine → vinylnitrene → 2*H*-azirine → methyl isocyanide → acetonitrile (Scheme 3). In the second pathway, vinylnitrene rearranges directly to acetonitrile via a 2,3 H transfer. In the two cases the rate-determining step in the reaction is the formation of vinylnitrene with an activation barrier of 75 kcal/mol. On the other hand, Kakimoto et al.[27] modeled the acetonitrile formation by one-step 1,3 H migration from keteneimine and found an activation energy of 96 kcal/mol, which is 21 kcal/mol higher than the one required for the 1,2 H migration. Finally, the activation barrier to directly obtain acetonitrile by decomposition of acetyl cyanide **1** is calculated to be 118 kcal/mol.[9]

In our experiments, the keteneimine and zwitterion are intermediate products. All these results suggest that the acetonitrile is obtained from keteneimine **6** irradiation by a 1,2 H migration process.

The 2*H*-azirine is not observed during irradiation of H_2C_2-NH **6**, and we can admit that the second pathway calculated by Doughty et al.,[26] is more consistent with our experimental results. By analogy, we can assume that H_2CNCH **5** yields the methyl isocyanide.

During the photolysis experiment at $\lambda > 180$ nm, the photolysis of **1** is the major pathway with regard to the photodecomposition of **2**. Indeed, as previously observed, the ketene:HCN complex is formed in greater amounts than the ketene:HNC complex. Thus, the fact that CH_3NC is formed in a greater amount than CH_3CN, despite the possible CH_3NC isomerization to CH_3CN, confirms that CH_3NC comes from the photolysis of **1** (Scheme 1).

Conclusion

During photolysis at $\lambda > 230$ nm, acetyl cyanide isomerizes to acetyl isocyanide **2**. The first reaction process is the elimination of HCN or HNC along with formation of ketene leading to ketene:HCN **3** and ketene:HNC **4** complexes from photolysis of acetyl cyanide and acetyl isocyanide, respectively. The 1:1 complexes between ketene and HCN or HNC were studied by DFT calculations. The most stable observed complexes were described by a linear structure. Irradiation at shorter wavelengths gives the same primary products and induces the photolysis of **3** and **4**. The ketene:HCN and ketene:HNC complexes yield, by decarbonylation process, the zwitterion H_2-CNCH and the keteneimine H_2C_2NH, respectively, trapped with CO molecules. In the last step, H_2CNCH gives by a 1,2 H migration methyl isocyanide, which isomerizes to acetonitrile. This last is the final reaction product, and it is also obtained by a 1,2 H migration from keteneimine H_2C_2NH. These experi-

mental data are in agreement with calculations performed in the ground state.[10]

Acknowledgment. The authors express their gratitude to F. Borget for helpful discussions. The theoretical section of this work was conducted with the assistance of "Centre Régional de Compétence en Modélisation de Marseille".

References and Notes

(1) Krisher, L. C.; Wilson, E. B. J. *Chem. Phys*. **1959**, *31*, 882.
(2) Sugie, M.; Kuchitsu, K. *J. Mol. Struct*. **1974**, *20*, 437.
(3) Heise, H. M.; Scappini, F.; Dreizler, H. *Z. Naturforsch*. **1976**, *31a*, 840.
(4) Bell, S.; Gurgis, G. A.; Lin, J.; Durig, J. R. *J. Mol. Struct*. **1990**, *238*, 183.
(5) Tate, B. E.; Bartlett, P. D. *J. Am. Chem. Soc*. **1956**, *78*, 5575.
(6) Okada, K.; Saito, K. *J. Phys. Chem*. **1995**, *99*, 13168.
(7) Bennet, R. N.; Jones, E.; Ritchie, P. D. *J. Chem. Soc*. **1956**, 2628.
(8) (a) So, S. P. *Chem. Phys. Lett*. **1997**, *270*, 363. (b) Ding, W. J.; Fang, W. H.; Liu, R. Z. *Chem. Phys. Lett*. **2002**, *351*, 9.
(9) Sumathi, R.; Nguyen, M. T. *J. Phys. Chem. A* **1998**, *102*, 412
(10) (a) Horwitz, R. J.; Fransisco, J. S.; Guest, J. A. *J. Phys. Chem. A* **1997**, *101*, 1231. (b) North, S. W.; Marr, A. J.; Furlan, A.; Hall. G. E. *J. Phys. Chem. A* **1997**, *101*, 9224. (c) Owrutsky, J. C.; Baronawski, A. P. *J. Chem. Phys*. **1999**, *111*, 7329. (d) Furlan, A.; Schels, H. A.; Huber, J. R. *J. Phys. Chem. A* **2000**, *104*, 1920.
(11) Lee, I. R.; Chung, Y. C.; Chen, W. K.; Wong, X. P. Cheng, P. Y. *J. Chem. Phys*. **2001**, *115*, 10656.
(12) Aoyama, J. I.; Sugihara, T.; Tabayashi, K.; Saito, K. *J. Chem. Phys*. **2003**, *118*, 6348.
(13) Hertenstein, U.; Hünig, S.; Reichelt, H.; Schaller, R. *Chem. Ber*. **1982**, *115*, 261.
(14) Piétri, N.; Jurca, B.; Monnier, M.; Hillebrand, M.; Aycard, J. P. *Spectrochim. Acta, Part A* **2000**, *56*, 157.
(15) Frisch, M. J.; Trucks, G. W.; Schlegel, H. B.; Scuseria, G. E.; Robb, M. A.; Cheeseman, J. R.; Zakrzewski, V. G.; Montgomery, J. A., Jr.; Stratmann, R. E.; Burant, J. C.; Dapprich, S.; Millam, J. M.; Daniels, A. D.; Kudin, K. N.; Strain, M. C.; Farkas, O.; Tomasi, J.; Barone, V.; Cossi, M.; Cammi, R.; Mennucci, B.; Pomelli, C.; Adamo, C.; Clifford, S.; Ochterski, J.; Petersson, G. A.; Ayala, P. Y.; Cui, Q.; Morokuma, K.; Malick, K. D.; Rabuck, A. D.; Raghavachari, K.; Foresman, J. B.; Cioslowski, J.; Ortiz, J. V.; Baboul, A. G.; Stefanov, B. B.; Liu, G.; Liashenko, A., Piskorz, P.; Komaromi, I.; Gomperts, R.; Martin, R. L.; Fox, D. J.; Keith, T.; Al-Laham, M. A.; Peng, C. Y.; Anayakkara, A. N.; Gonzalez, C.; Challacombe, M.; Gill, P. M. W.; Johnson, B.; Chen, W.; Wong, M. W.; Andres, J. L.; Gonzalez, C.; Head-Gordon, M.; Replogle, E. S.; Pople, J. A. *Gaussian 03*; Gaussian, Inc.: Pittsburgh, PA, 1998.
(16) Moore, C. B.; Pimentel, G. C. *J. Chem. Phys*. **1963**, *38*, 2816.
(17) (a) Satoshi, K.; Takayanagi, M.; Nakata, M. *J. Mol. Struct*. **1997**, *365*, 413. (b) King, C. M.; Nixon, E. R. *J. Chem. Phys*. **1968**, *48*, 1685.
(18) Milligan, D. E.; Jacox M. E. *J. Chem. Phys*. **1967**, *47*, 278.
(19) (a) Maier, G.; Schlidt, C.; Reisenamer, H. P.; Endlein, E.; Becker, D.; Eckwert, J.; Hess, B. A.; Schaad, L. *J. Chem. Ber*. **1993**, *126*, 2337. (b) Jacox, M. E. *J. Phys. Chem. Ref. Data* **1998**, *27*, 115.
(20) (a) Jacox, M. E.; Mulligan, D. E. *J. Am. Chem. Soc*. **1963**, *85*, 278. (b) Jacox, M. E. *Chem. Phys*. **1979**, *43*, 157.
(21) Dubost, H.; Abouab-Mangum, L. *Chem. Phys. Lett*. **1972**, *17*, 269.
(22) (a) Freedman, T. B.; Nixon, E. R. *Spectrochim. Acta, Part A* **1972**, *28*, 1375. (b) Jacox, M. E. *J. Mol. Spectrosc*. **1978**, *71*, 369.
(23) Pietri, N.; Allouche, A.; Aycard, J. P.; Chiavassa, Y. *J. Phys. Chem*. **1997**, *101*, 1093.
(24) Tidwell, T. T. *Ketenes*; Wiley-Interscience: New York, 1995.
(25) Hochstrasser, R.; Wirz, J. *Angew. Chem., Int. Ed. Engl*. **1990**, *29*, 411.
(26) Doughty, A.; Bacskay, G. B.; Mackie, J. C. *J. Phys. Chem*. **1994**, *98*, 13546.
(27) Kakumoto, T.; Ushrirogouchi, T.; Saito, K.; Imamura, A. *J. Phys. Chem*. **1987**, *91*, 183.